metals

MDPI

Article

Application of Tungsten Nanopowder in Manual Metal Arc, Metal Inert Gas, and Flux-Cored Arc Welding Surfacing

Evgenii Zernin *, Ekaterina Petrova, Alexander Scherbakov, Ekaterina Pozdeeva and Anatolij Blohin

World-Class Research Center "Advanced Digital Technologies", State Marine Technical University, Saint Petersburg 190000, Russia
* Correspondence: zernin@smtu.ru

Abstract: The main directions and fields of the application of metal nanopowders in joining technologies are considered. Based on this analysis, the purpose of this research was to determine the effect of tungsten nanopowder on the structure and properties of the deposited metal. In order to increase the efficiency of using tungsten nanopowder for modification, it is necessary to ensure the introduction of nanopowder into the low-temperature zone of the molten metal during surfacing. To study the metal, microstructural analysis was performed, and the microhardness of the deposited joint was determined. On the basis of the conducted studies, a change in the structure of the deposited metal and an increase in mechanical properties were revealed. A conclusion is made about the effect of tungsten nanopowder on the metal modification process during manual metal arc, metal inert gas, and flux-cored arc welding. Based on the conducted studies, it was found that the introduction of tungsten nanopowder into the low-temperature zone of the molten metal ensures the modification of the surfacing and induces an increase in the microhardness of the deposited metal. At the same time, grains of polyhedral morphology are formed at the surface, and the structure of oriented dendrites at the boundary of fusion with the base metal is also revealed, showing the peculiarities of the distribution of microhardness in various surfacing methods. The minimum and maximum values of microhardness depend not only on the nanopowder but also on the method of its introduction into the molten metal.

Keywords: nanopowder; surfacing; microstructure; mechanical properties

Citation: Zernin, E.; Petrova, E.; Scherbakov, A.; Pozdeeva, E.; Blohin, A. Application of Tungsten Nanopowder in Manual Metal Arc, Metal Inert Gas, and Flux-Cored Arc Welding Surfacing. *Metals* **2024**, *14*, 1376. https://doi.org/10.3390/met14121376

Academic Editors: Matteo Benedetti and Frank Czerwinski

Received: 30 October 2024
Revised: 27 November 2024
Accepted: 30 November 2024
Published: 2 December 2024

1. Introduction

The field of materials science in the 21st century is mainly focused on the development of nanomaterials and nanopowders. One of the main advantages of such materials is that their structure improves the performance of steel and non-ferrous metal products [1]. The performance is affected by parameters such as material removal rate, surface roughness, and electroerosion cladding time [2].

A significant amount of scientific research is required to increase the durability and operational reliability of metal structures and obtain new metals, as well as the massive introduction of new advanced technologies into industrial production. One of the priority areas is the use of nanopowders of various metals and their compounds. Such materials contribute to a significant increase in production efficiency in mechanical engineering, metallurgy, energy, construction, etc. [3–5].

Considerable attention has been paid to the use of nanopowders of refractory metals in welding, surfacing, and spraying in recent years. One of the main tasks solved when using nanopowders is the modification of the deposited metal. This allows for controlling the structure and properties of the deposited layer, which, in turn, allows us to obtain products with specified performance indicators.

Modern publications note the significant role of modification with nanopowders as a factor in controlling the structure and properties of the deposited metal. The main part

of the research has been carried out in relation to connecting technologies for low-alloy steels. In this case, inclusions formed in the deposited metal in the form of oxides, carbides, and nitrides are considered because of chemical compounds of the corresponding elements during the crystallization process. Inclusions are formed in different size ranges from 1 μm to nanosize [6]. Thus, in work [7], the influence of the size of non-metallic inclusions on the structural formation, composition, and distribution features of non-metallic inclusions in the presence of various oxides was studied.

In other cases, the formation of non-metallic inclusions is a consequence of the introduction of nanooxides or nanocarbides into the weld pool [8]. In all cases, the positive role of nanodisperse inclusions of a certain composition and distribution density on the structure and properties of welded joints is noted.

Obtaining a modified structure by welding makes it possible to improve the mechanical properties as a whole compared to those of a structure with coarse grains [6] and to improve corrosion characteristics due to the introduction of ultra- and nanodisperse mi-croadditives of rare and alkaline earth elements [9].

One of the disadvantages of modifying the deposited metal is that during the welding process, the temperature in the arc zone exceeds the melting point of many nanostructured powders, which leads to their dissociation and the subsequent dissolution of the products in the melt of the weld pool. In this regard, most studies are devoted to studying the effect of tungsten carbide on the properties of refractory alloys, as it has increased thermal stability, higher values of the elastic modulus, and a lower coefficient of thermal expansion compared to carbides of other metals [10,11]. The modification technology is proposed for a joint welded with aluminum nanooxides through double-coated electrodes with aluminum oxide nanoadditive [12]. Aluminum oxide passes into the liquid bath and is homogeneously distributed without significant accumulations, while complex inclusion (aluminum, manganese, silicon, oxygen, and carbon) occurs, and the added nanooxides accelerate the release of other oxides and sulfides. Nanoparticles of titanium carbide [13] and aluminum oxide [14] are used for better-quality, unbreakable connections.

Also, the mechanical properties, chemical composition, microstructure, geometrical parameters, and hardness of welded joints are influenced by welding modes [15,16], namely, voltage, current strength, welding speed, and the distance between the contact tip and plate [17,18]; the modification of the liquid welding bath with metal oxides through the electrode [19]; the use of titanium oxide introduced into the coating of welding electrodes [20]; nanoparticles that are incorporated into fluxes [21]; filler size; and brazing temperatures [22,23]. New brazing applications, including the latest entropy-modified fillers for brazing various structural and process areas, are also reviewed [24].

For example, flux-cored wires contain various nanostructured modifier powders in different percentages for TIG surfacing [25]. The nanomodified coatings are applied by cladding on structural steel specimens. The addition of particles is realized in the low-temperature region of the weld pool, thus preventing them from overheating. The surface layers deposited by the developed wires have increased hardness, wear resistance, and corrosion resistance. The addition of nanoscale powders to the hardened coating im-proves mechanical properties, wear resistance, and corrosion resistance [5]. The addition of yttrium oxide allows a carbide coating with improved mechanical properties to be obtained [26]. The positive effect on the cladding structure is solved by the introduction of nanostructured aluminum oxohydroxide fibers into the melt of the welding pool through the shielding (transporting) gas [27].

The use of nano- and ultradisperse materials in connecting technologies is mainly aimed at controlling the structure and properties of permanent connections. Based on the analysis of global experience in the use of nanomaterials in joining technologies and according to the data presented in [28], the systematization of methods for using nano- and ultrafine powders in fusion welding (surfacing) was carried out (Figure 1).

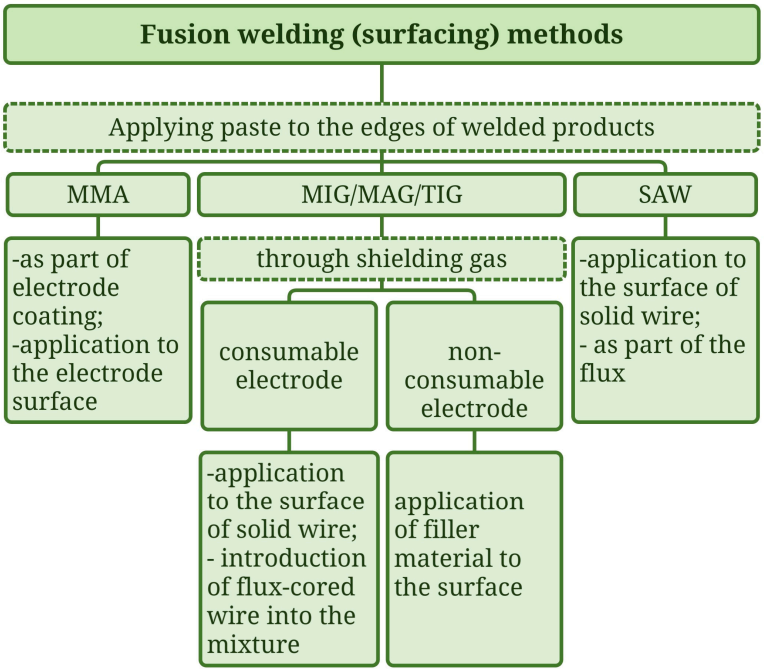

Figure 1. Application of nano- and ultrafine powders in arc welding and surfacing: MMA—manual metal arc; MIG—metal inert gas; MAG—metal active gas; TIG—tungsten inert gas; SAW—submerged arc welding.

It should be noted that with most fusion welding (surfacing) methods, it is possible to introduce such powders into the welding zone through specialized pastes that are applied to the edges of the products being welded. And during MIG/MAG/TIG welding (surfacing), this can be performed through shielding gas. A review of the use of nano- and ultradisperse materials to control the structure and properties of metals in joining technologies shows that technological solutions are actively developing in this area. Such solutions are based, first of all, on the creation of new materials for welding, soldering, and surfacing. The development of methods for welding and surfacing with flux-cored wire, which includes nano- and ultrafine materials, is promising.

At present, a promising direction in the development of surfacing and recovery technologies is the use of nanopowders in the composition of combined welding consumables. The fundamental possibility of forming the surface of products with desired properties should be noted as the main advantage of such materials. The practical application of nanopowders in the composition of welding consumables is still a rather complex and time-consuming process.

Depending on the technique for surfacing layers with desired properties, the following methods of introducing nanopowders into the liquid melt of the weld pool can be considered:

- Coating piece electrodes in manual arc surfacing;
- Shielding (transporting) gas during mechanized surfacing with solid wire;
- Introducing flux-cored wire used for surfacing into the charge.

This paper considers all three listed methods of surfacing using nanopowders to reveal the trends in the formation of the structure and properties of the deposited metal.

Since the structure and properties of the deposited metal depend significantly on the surfacing method, the purpose of this work is to determine the effect of tungsten nanopowder on the microstructure and hardness of the deposited metal in the following surfacing methods: MMA (manual metal arc), MIG (metal inert gas), and FCAW (flux-cored arc welding) surfacing.

The peculiarity of the selected surfacing techniques and the methods of their implementation is that the W nanopowder does not fall into the zone of the welding bath with

the highest temperature (under the welding arc). This ensures the preservation of the W nanopowder.

2. Materials and Methods

Various methods and techniques are used to produce nanopowders [29–40]. It should be noted that tungsten nanopowder was initially obtained using the technology described in [29,30]. This nanopowder was used in the three surfacing methods considered in this paper.

One of the main tasks for the practical application of nanopowders in welding consumables is to ensure a uniform distribution of such powders over the volume of the welding consumables: stick electrode coatings, flux-cored wire charge, etc.

All the studies in this paper were conducted on the basis of planning a factorial experiment.

With the selected methods (MMA, MIG, and FCAW), surfacing was performed on a base made of 10XCND low-carbon steel. The thickness of the base metal was 10 mm.

For MMA surfacing, UONI-13/45 electrodes were used. The diameter of each electrode was 3 mm. During FCAW surfacing, PP-AN170M wire was used as a surfacing material. The same materials were used for a prototype to produce wire with the addition of W nanopowder. The diameter of the powder wire was 3.4 mm.

High-purity argon gas was used for MIG and FCAW.

The following equipment was used for surfacing: DC power supply for welding (MMA, MIG, and FCAW) and an automatic welding head (MIG and FCAW). In all cases, direct current was used. The welding mode for MMA was as follows: welding current 90–94 A; arc voltage 20–22 V. The welding mode for MIG and FCAW was as follows: welding current 320–340 A; arc voltage 32–34 V.

The variable parameters of the surfacing process were selected in accordance with the recommendations and data provided in [1,7,9,11,15,17,19]. The original modification method for MIG was also used. The surfacing modes were assumed to be fixed, depending on the diameter of the wire (MIG and FCAW surfacing) or electrode (MMA surfacing). The thickness of the deposited layer in all cases (MMA, MIG, and FCAW surfacing) was 3.4 mm.

Tungsten nanopowder was added to the powder wire (FCAW surfacing) or to the coated electrode (MMA surfacing) at a rate of 1 g per 1 m. Additionally, for FCAW, the tungsten content in the powder wire was changed from 0 to 1 g per 1 m of wire in increments of 0.2 g per 1 m of wire. During MIG surfacing, the consumption of tungsten nanopowder was 1 g per 1 m^3 of argon.

The schemes of the surfacing processes are shown in Figures 2–4. In all three schemes, 4 is the low-temperature surfacing zone (1450–2000 °C), and 5 is the high-temperature surfacing zone (above 2000 °C).

The principle of operation (Figure 2) is as follows: The metal rod of the electrode and the main coating of the electrode are melted and then sent to the high-temperature surfacing zone 5. The additional electrode coating containing W nanopowder is melted and then sent to the low-temperature surfacing zone 4.

The principle of operation (Figure 3) is as follows: During surfacing, wire 3 is additionally supplied to wire 1. The additional powder wire containing W nanopowder is fed into the low-temperature surfacing zone 4. This method of wire feeding exerts a positive effect, which is confirmed in work [41].

The principle of operation (Figure 4) is as follows: A transporting gas is supplied through nipple 1 and, after passing through the axial channel of the injector (3), enters the mixing chamber (6) and creates a discharge of 11–40 kPa in the channel (9). This leads to the suction of nanoparticles from the storage unit (7). The concentration of nanoparticles in the transporting gas is adjusted by an adjustment valve (8). To prevent ingress into the transporting gas, an ultrafine air powder is supplied to the storage unit (7) through nipple 2 with argon gas. Then, the Ar + nano W mixture is fed into the low-temperature surfacing zone 4.

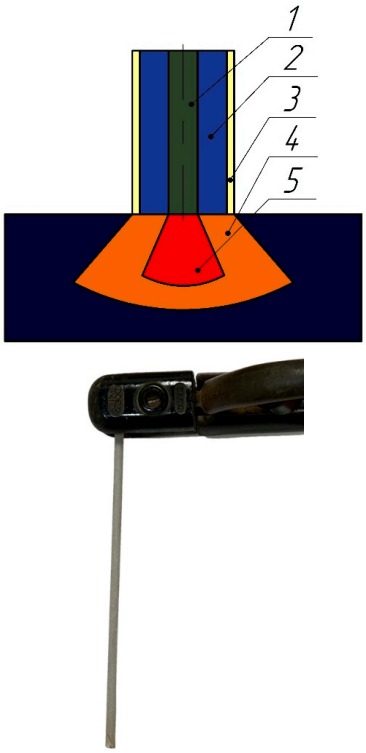

Figure 2. MMA surfacing scheme: (1)—the metal rod of the electrode; (2)—the main coating of the electrode; (3)—the additional electrode coating containing W nanopowder; (4)—the low-temperature surfacing zone; (5)—the high-temperature surfacing zone.

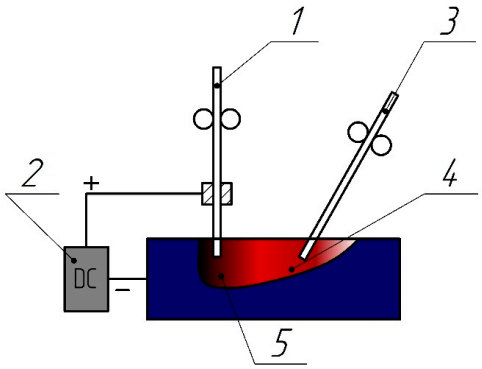

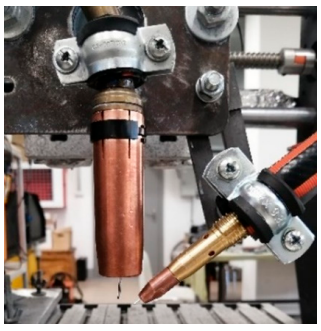

The device for implementing the process

Figure 3. FCAW surfacing scheme: (1)—the main powder wire; (2)—the power supply for welding; (3)—the additional powder wire containing W nanopowder; (4)—the low-temperature surfacing zone; (5)—the high-temperature surfacing zone.

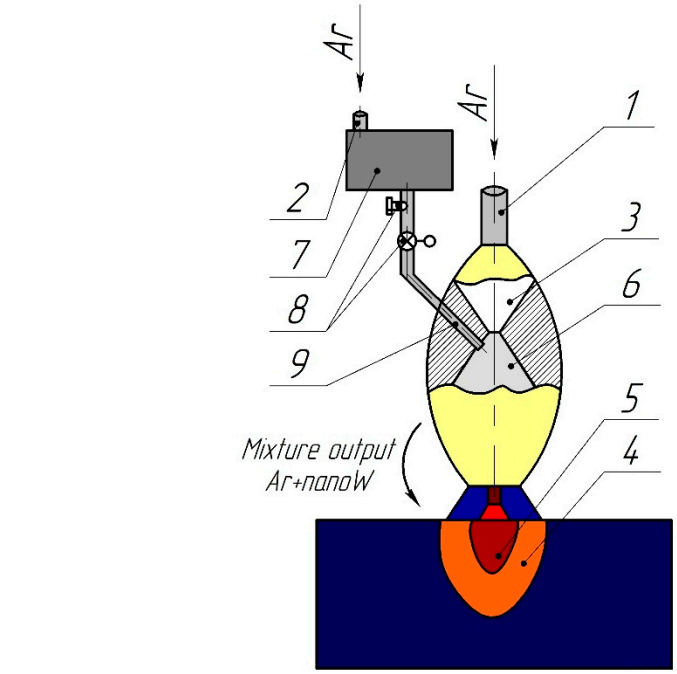

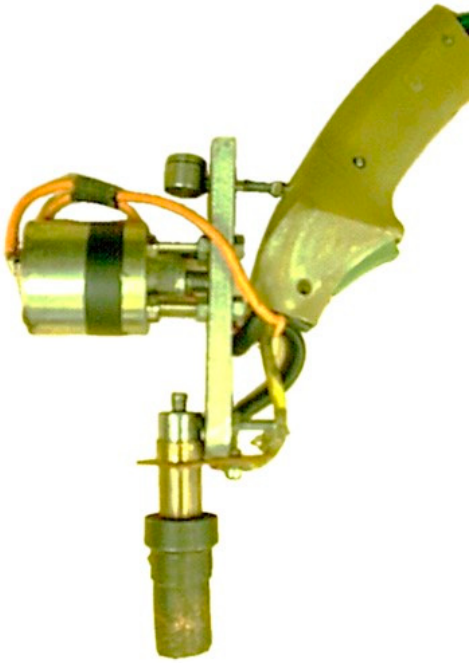

The device for implementing the process

Figure 4. MIG surfacing scheme: (1) and (2)—the nipples; (3)—the injector; (4)—the low-temperature surfacing zone; (5)—the high-temperature surfacing zone; (6)—the mixing chamber; (7)—the nanopowder storage; (8)—the valve with a sensor for adjusting the concentration of nanopowder in the transporting gas; (9)—the channel for the primary mixture of Ar + nano W.

After surfacing, samples were cut out to study the microstructure and determine microhardness. The scheme for studying the microstructure and determining the microhardness is shown in Figure 5. The microhardness and microstructure were determined from the outer surface of the deposited metal in the direction of the substrate in 0.5 mm increments.

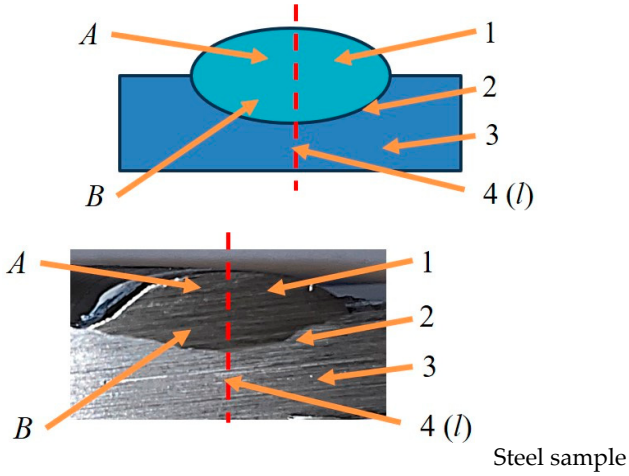

Figure 5. Scheme of a section for studying the microstructure of the deposited metal: (1)—the deposited metal; (2)—the fusion line of the deposited metal and the substrate; (3)—the substrate; (4)—the microhardness measurement line (*l*); (*A*)—the upper layer of the deposited metal (the area of "granular" dendrites); (*B*)—the lower layer of the deposited metal (the area of oriented dendrites).

The microstructure and phase composition of samples were determined by optical metallography with digital camera image registration after selective etching. The analysis was carried out using optical metallography on a Neophot-21 microscope (Carl Zeiss, Jena, Germany) with image registration using a Genius VileaCam digital camera. The grain size was determined in accordance with [42].

The microhardness of the deposited and base metals was determined using a PMT-3M microhardness meter by pressing a Vickers diamond tip with a square-base four-sided pyramid into the test material and reviewing the geometric and mechanical similarity of the prints as the indent deepened under the load. For the measurement of microhardness, the measurement step was 0.5 mm at a load of P = 0.98 N.

Microstructure and microhardness were studied using five samples for each surfacing method. At the same time, the microhardness was determined three times in identical places in each of the five samples.

3. Results

The microstructural analysis of deposited layers presented in Figure 6 was carried out in comparison with surfacing, with electrodes taken as a basis (without the addition of tungsten nanopowder).

Microstructural analysis showed that when tungsten nanopowder was introduced into the combined electrode coating, the structure of the deposited metal became finer-grained, both in the crystallized zone of small crystals and in the zone of columnar crystals. The average size was reduced by 35%, the average transverse size was reduced by 61%, and the average size of branches was reduced by 40%.

The evaluation of the mechanical properties showed that during surfacing in the presence of tungsten nanopowder, the microhardness of the deposited layer in the upper layer *A* increased by 1.3 fold and that in the lower layer *B* by 1.4 fold (Figure 7). This allows for conclusions about the increase in the strength characteristics of the deposited metal.

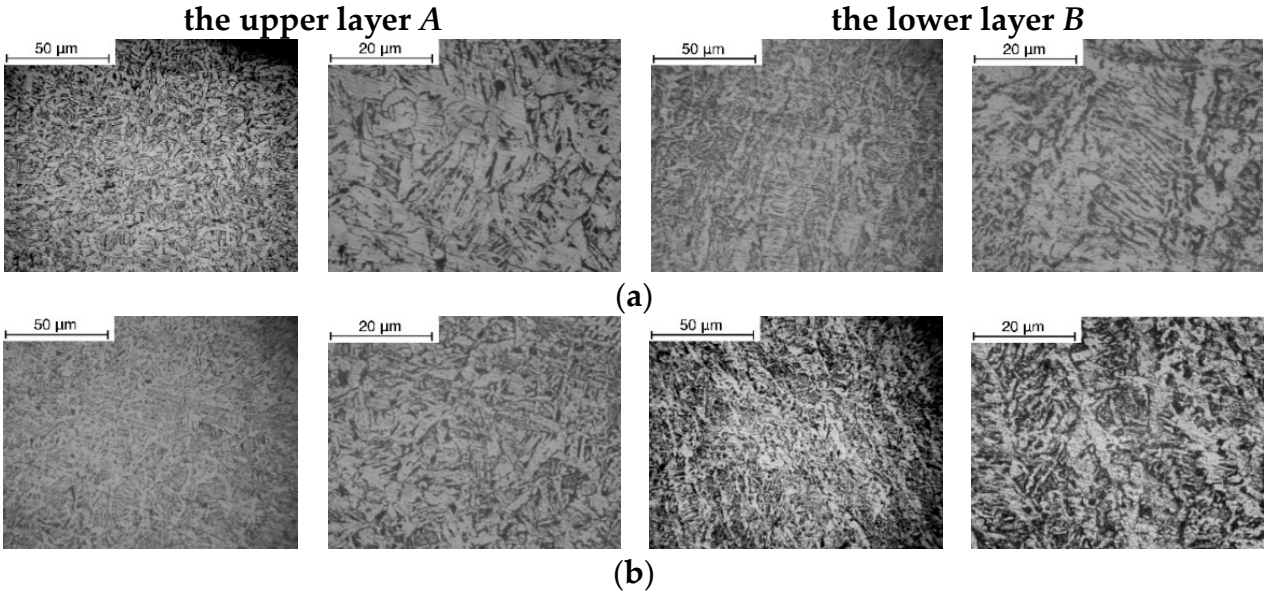

Figure 6. MMA. Microstructure of deposited layers: (**a**)—original electrode; (**b**)—electrode with combined coating containing tungsten nanopowder.

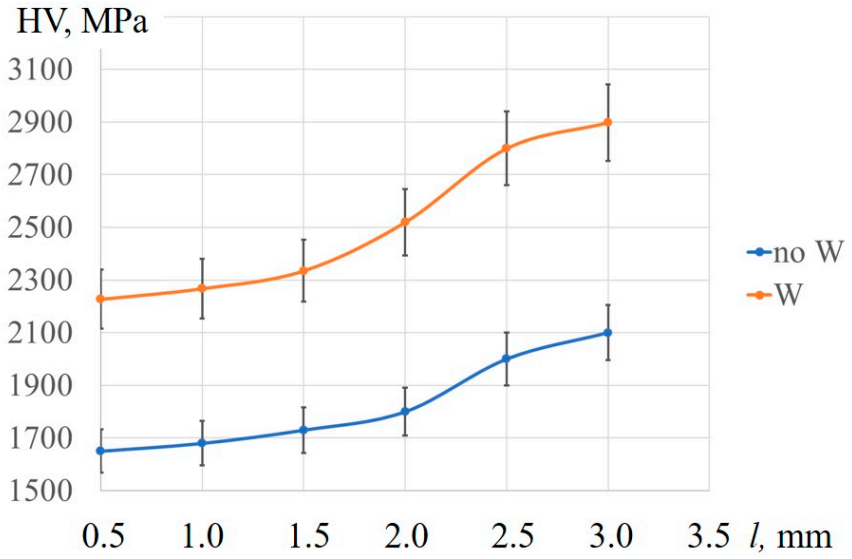

Figure 7. MMA. Microhardness of the deposited metal: l = 0.5; 1.0; 1.5 mm—response of the upper layer A; l = 2.0; 2.5; 3.0 mm—response of the upper layer B (Figure 6).

One of the representatives of combined surfacing materials is flux-cored wire, which makes it possible to obtain practically any composition of the deposited metal and can also be used for surfacing steels and alloys with special properties. The structure and properties of the deposited metal can be controlled by adding appropriate components to the charge. Such components can be nanopowders and nanomaterials.

Studies of the microstructure of the deposited FCAW surfacing of various samples showed that they all had a similar structure and were characterized by two distinct areas: the area of "grain" dendrites and the area of differently oriented dendrites (Figure 8).

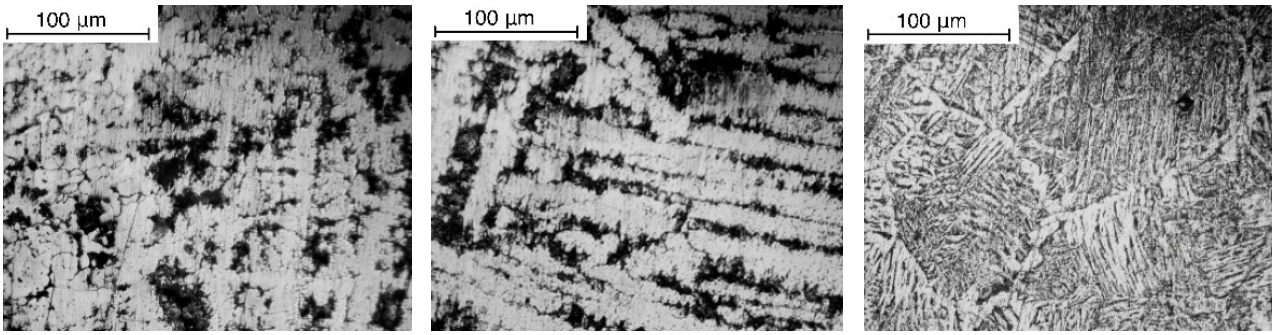

Figure 8. FCAW. The microstructure of the deposited metal: (**a**) area of "grain" dendrites (l = 0.5; 1;1.5 mm); (**b**) region of differently oriented dendrites (l = 2; 2.5; 3 mm); (**c**) base metal.

However, despite the similar structure, with an increase in the content of nanopowder in the wire charge, the grain size decreased. The experimental data on the change in grain size depending on the concentration of tungsten nanopowder in the wire charge are shown in Figure 9.

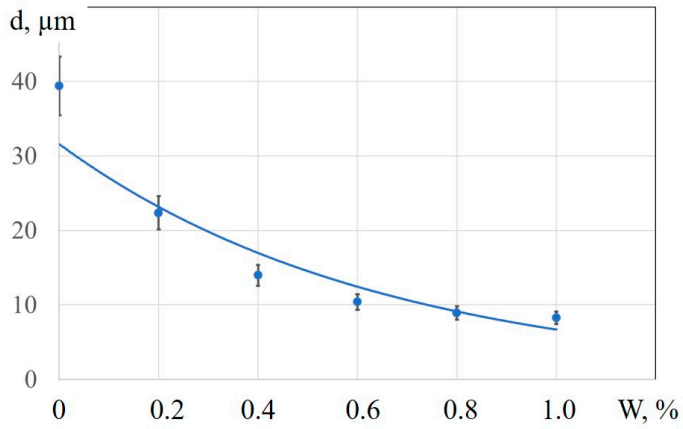

Figure 9. Effect of tungsten nanopowder concentration on grain size.

In this case, the particles of tungsten nanopowder serve as ready crystallization centers, functioning as a weld metal modifier.

The experimental data for measuring microhardness are shown in Figure 10.

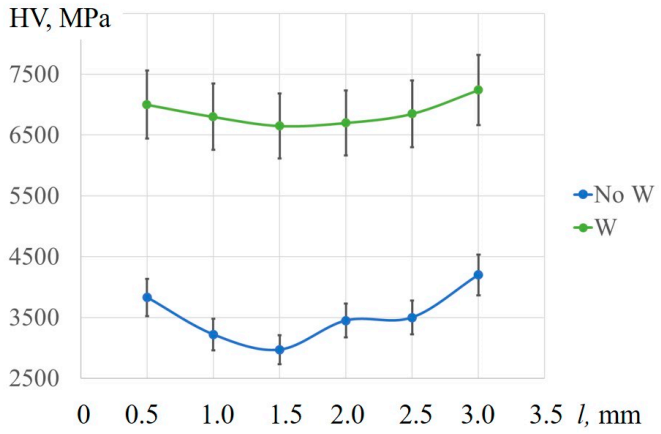

Figure 10. FCAW. Distribution of the microhardness of the deposited metal.

At the same time, microhardness indices are slightly higher at the fusion boundary, which is due to the different heat supplied during the crystallization of the deposited metal into the surrounding atmosphere and into the base metal.

The use of tungsten nanopowder as part of an additional wire additive makes it possible to increase the microhardness and, consequently, the strength properties of the deposited layers.

The microstructures of individual areas of surfacing without the addition of tungsten and with tungsten in the carrier gas are shown in Figure 11.

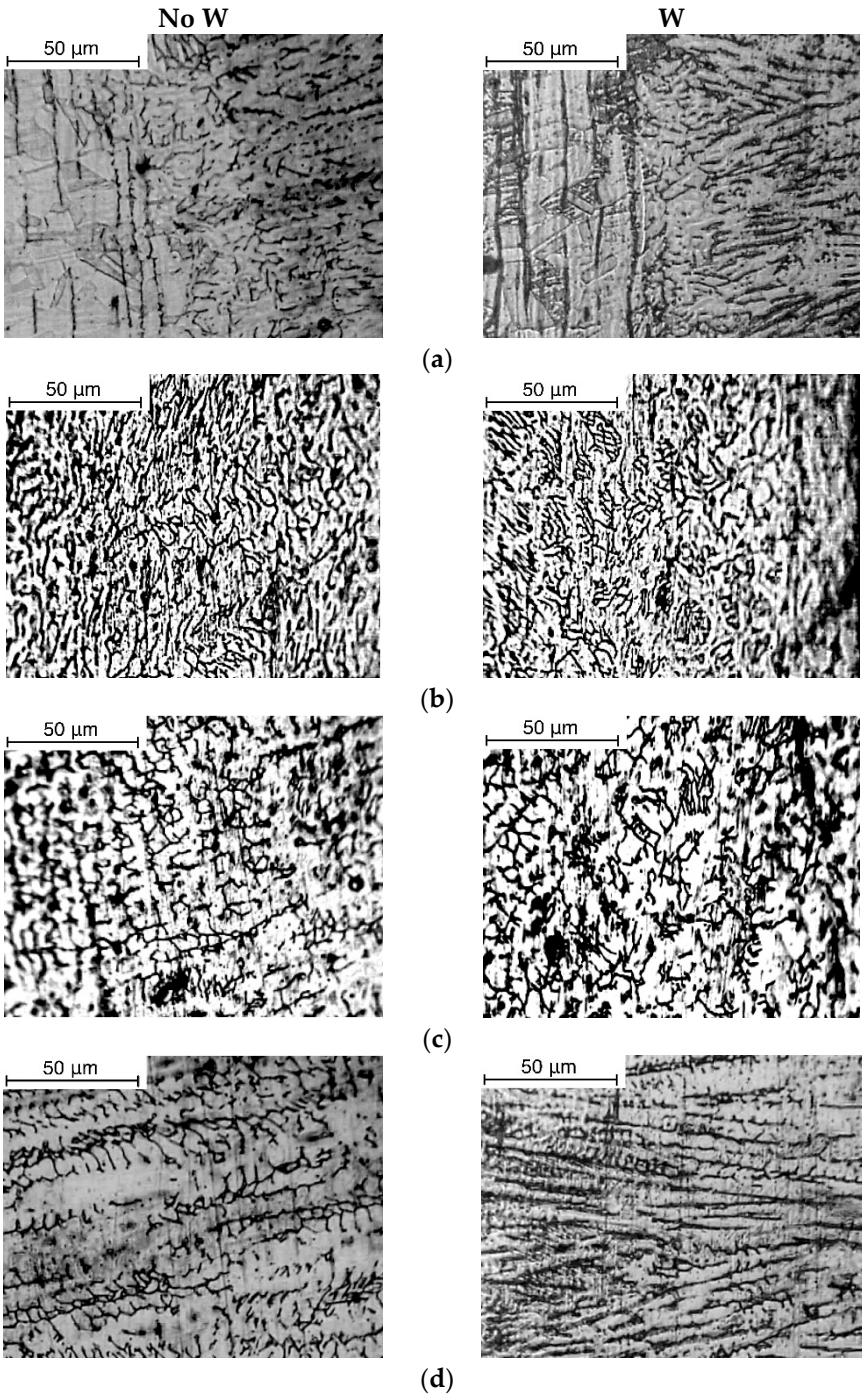

Figure 11. MIG. The microstructure of the deposited layer: (**a**) the boundaries of fusion of the deposited metal and the substrate; (**b**) a layer of polyhedral grains (I = 0.5 and 1 mm); (**c**) a layer of unoriented dendrites (I = 1.5 and 2.5 mm); (**d**) a layer of oriented dendrites (I = 2.5 and 3 mm).

Analysis of the microstructure showed that at the fusion boundary (Figure 11a), there was a smooth transition from the dendritic structure of the deposited metal to the polyhedral grain structure of the heat-affected zone.

The layer directly adjacent to the free surface can be characterized as a layer with a polyhedral grain structure. In this layer, along with randomly located (unoriented) dendrites, polyhedral grains are observed. This layer is less pronounced in sample No W. In sample W, the "grain" layer is more pronounced. Gains with polyhedral morphology are clearly visible here, which alternate with islands of short, unoriented dendrites.

The main microstructural components of the next layer are relatively short, highly branched dendrites with no preferred orientation. This layer is again less pronounced in sample No W. The layer of unoriented dendrites is better expressed in sample No W. Whereas in sample 1, the dendrites form an almost continuous network, in sample W, islands of the free surface are observed. A layer of short, strongly branched dendrites that do not have a predominant orientation smoothly passes into the next layer of oriented dendrites.

The orientation of the long axes of the dendrites in the layer under consideration is normal to the fusion boundary, i.e., along the direction of the heat flow from the deposited metal to the substrate.

More branched and thicker dendrites are observed in sample No W. In this case, the average width of the dendrites is 15 μm, while in sample W, the dendrites are thin and slightly branched with an average width of 11 μm. The thickness in both cases is comparable and is about 1.5 μm.

The deposited metal has a layered structure, which is due to a change in heat removal conditions while moving deeper into the liquid pool. Near the free surface, heat removal is weak; therefore, crystallization proceeds according to the mechanism of formation of polyhedral grains; dendrites practically do not have time to form. In the rest of the weld metal, typical dendritic crystallization occurs. Approximately half of the deposited metal volume is occupied by oriented dendrites. There is also a layer of unoriented dendrites. According to generally accepted ideas, the less the dendritic structure of the deposited metal is manifested and the less coarse the structure of the dendrites, the better the mechanical properties of the deposited layers. From this standpoint, the deposited metal of the sample surfaced in argon with a solid wire is inferior to that of the samples surfaced in argon with a solid wire with the addition of tungsten nanopowder.

The microhardness of two samples was measured along the deposit axis perpendicular to the free surface to assess the change in the mechanical characteristics of the deposited metal. Experimental data are presented in Figure 12.

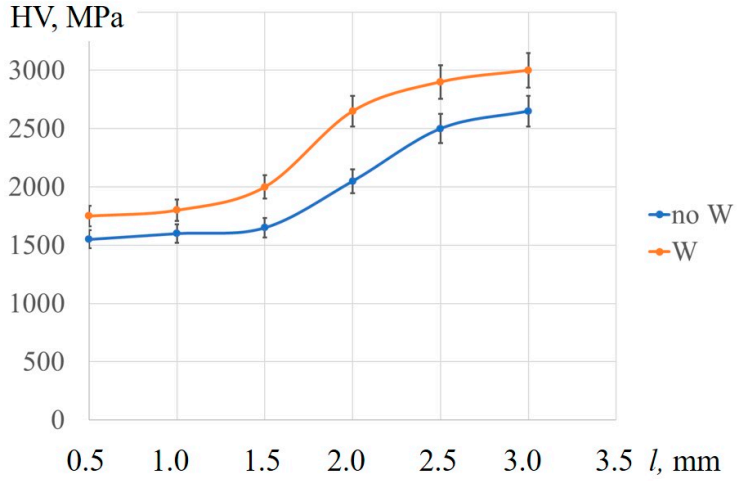

Figure 12. MIG. Microhardness of the deposited metal.

The microhardness of the layers naturally increases with the transition to the base metal. The hardness in the deposited metal with tungsten nanopowder is higher than that in the specimen deposited without the use of tungsten nanopowder. Thus, the experimental data confirm the change in structure formation and the increase in the mechanical properties of the metal deposited in the presence of tungsten nanopowder.

4. Discussion

An analysis of the experimental data shows that for all methods of layer surfacing in the presence of tungsten nanopowder, the morphology of the deposited metal changes. This statement does not contradict the data presented in [3,6–8,12,19–21].

The use of tungsten nanopowder unequivocally leads to a more balanced and finely dispersed structure of the deposited metal, with a simultaneous increase in microhardness.

The nature of the distribution of microhardness also has a similar character—the highest values are observed near the fusion zone, and the lowest values are near the free surface. The absolute value of microhardness is primarily determined by the source material for surfacing.

In all cases, tungsten nanopowder particles serve as ready-made crystallization centers, functioning as a weld metal modifier. By adjusting the concentration of tungsten in the composition of materials for surfacing and in the process of obtaining layers, it is possible to control the structure of the deposited metal.

The properties of the deposited metal (surfacing layers) mainly depend on the geometric parameters and the shape of the dendrites, the formation of which occurs because of the crystallization of the weld pool. This is confirmed by the data obtained in works [43–46].

The degree of influence of tungsten nanopowder differs with different surfacing methods. The greatest effect is observed when the modifier is introduced into the composition of the charge of additional additive wire during the surfacing of powder material. The most effective is the use of nanopowder in FCAW surfacing. In this case, the additive flux-cored wire, the charge composition of which includes tungsten nanopowder, is fed into the tail part of the weld pool. The additive wire is melted in a stream of superheated liquid metal of the weld pool directed from under the arc to the tail section. The nanopowder from the molten additive wire enters the tail of the weld pool without passing through the arc gap, i.e., practically without loss; it passes into the liquid metal of the weld pool, mixes with it, and provides additional crystallization centers during the formation of a grain in the microstructure of the deposited metal, i.e., modifying the structure of the deposited metal. Powder nanoparticles do not melt in a liquid weld pool.

The smallest effect is achieved when using combined coated stick electrodes.

5. Conclusions

The application of tungsten nanopowder during surfacing (MMA, MIG, FCAW) shows its effectiveness.

The use of nanomaterials to control the structure and properties of metals in surfacing and other connecting technologies shows that there is an active development of technological solutions in this area. Such solutions are based primarily on the creation of new materials—electrodes and powder wires. The development of welding and surfacing methods with a powder wire, which will include nanopowders, is promising. As a result, it is possible to increase the performance of the deposited layers based on the use of nano powders. To achieve this goal, it will be necessary to solve the following scientific and practical tasks:

1. To develop scientifically based technological solutions for the use of nanopowders in the composition of the powder wire charge to improve the properties of the deposited layers.
2. To investigate the macro- and microstructure of surfaces obtained with the additional introduction of nanopowders into the welding bath in order to obtain surface layers of steels and alloys with special performance characteristics.

3. To investigate the effect of the use of nanopowders on improving the mechanical, physical, chemical, technological, and operational performance of non-ferrous metal compounds and alloys based on them.
4. To develop the application of nanotechnology in the field of composite material bonding.

Author Contributions: Conceptualization, E.Z. and E.P. (Ekaterina Petrova); methodology, E.Z. and E.P. (Ekaterina Petrova); software, E.P. (Ekaterina Petrova); validation, E.Z., E.P. (Ekaterina Petrova) and A.S.; formal analysis, E.P. (Ekaterina Pozdeeva) and A.B.; investigation, E.P. (Ekaterina Pozdeeva) and A.B.; resources, E.P. (Ekaterina Petrova) and A.S.; data curation E.Z. and E.P. (Ekaterina Petrova); writing—original draft preparation, E.P. (Ekaterina Pozdeeva) and A.B.; writing—review and editing, E.Z. and E.P. (Ekaterina Petrova); visualization, A.S., E.P. (Ekaterina Pozdeeva) and A.B.; supervision, E.Z.; project administration, E.Z.; funding acquisition, E.P. (Ekaterina Pozdeeva) and A.B. All authors have read and agreed to the published version of the manuscript.

Funding: The research was partially funded by the Ministry of Science and Higher Education of the Russian Federation as part of the world-class Research Center program Advanced Digital Technologies (contract No. 075-15-2022-312 dated 20 April 2022).

Data Availability Statement: The raw data supporting the conclusions of this article will be made available by the authors on request.

Conflicts of Interest: The authors declare no conflict of interest.

References

1. Markashova, L.; Berdnikova, O.; Alekseienko, T.; Bernatskyi, A.; Sydorets, V. Nanostructures in Welded Joints and Their Interconnection with Operation Properties. In *Advances in Thin Films, Nanostructured Materials, and Coatings*; Lecture Notes in Mechanical, Engineering; Pogrebnjak, A.D., Novosad, V., Eds.; Springer: Singapore, 2019. [CrossRef]
2. Saha, A.; Mondal, S.C. Statistical Analysis and Optimization of Process Parameters in Wire Cut Machining of Welded Nanostructured Hardfacing Material. *Silicon* **2019**, *11*, 1313–1326. [CrossRef]
3. Galevskii, G.V.; Rudneva, V.V.; Yurkova, E.K. Nanomaterials and nanotechnologies: Assessment, tendencies, and forecasts. *Russ. J. Non-Ferr. Met.* **2007**, *48*, 157–160. [CrossRef]
4. Pal, K.; Mohan, M.M.; Thomas, S. Dynamic application of novel electro-optic switchable device modulation by graphene oxide dispersed liquid crystal cell assembling CdS nanowires. *Org. Electron. Phys. Mater. Appl.* **2016**, *39*, 25–37. [CrossRef]
5. Reisgen, U.; Balashov, B.; Stein, L.; Geffers, C. Nanophase hardfacing new possibilities for functional surfaces. *Mater. Sci. Forum* **2010**, *638–642*, 870–875. [CrossRef]
6. Wang, J.-Y.; Chang, T.-C.; Chang, L.-Z.; Lee, S. Effect of Al and Mn Content on the Mechanical Properties of Various ECAE Processed Mg-Li-Zn Alloys. *Mater. Trans.* **2006**, *47*, 971–976. [CrossRef]
7. Seo, J.S.; Kim, J.; Lee, C. Effect of Ti addition on weld microstructure and inclusion characteristics of bainitic GMA welds. *ISIJ Int.* **2013**, *53*, 880–886. [CrossRef]
8. Vanovsek, W.; Bernhard, C.; Fiedler, M.; Posch, G. Influence of aluminum content on the characterization of microstructure and inclusions in high-strength steel welds. *Weld. World* **2013**, *57*, 73–83. [CrossRef]
9. Klimpel, A.; Kik, T. Erosion and abrasion wear resistance of GMA wire surfaced nanostructural deposits. *Arch. Mater. Sci. Eng.* **2008**, *30*, 121–124.
10. Zhu, Y.; Yukimura, K.; Ding, C.X.; Zhang, P.Y. Tribological properties of nanostructured and conventional WC-Co coatings deposited by plasma spraying. *Thin Solid Film.* **2001**, *388*, 277–282. [CrossRef]
11. Wu, P.; Du, H.M.; Chen, X.L.; Li, Z.Q.; Bai, H.K.; Jiang, E.Y. Influence of WC particle behavior on the wear resistance properties of Ni-WC composite coatings. *Wear* **2004**, *257*, 142–147. [CrossRef]
12. Chen, C.; Peng, H.; Liu, R.; Li, Y.; Zhao, P. Research on inclusions in low alloy steel welds with nano alumina addition. *J. Comput. Theor. Nanosci.* **2012**, *9*, 1533–1536. [CrossRef]
13. Sokoluk, M.; Cao, C.; Pan, S.; Li, X. Nanoparticle-enabled phase control for arc welding of unweldable aluminum alloy 7075. *Nat. Commun.* **2019**, *10*, 98. [CrossRef] [PubMed]
14. Praveen, A.S.; Arjunan, A. Effect of nano-Al_2O_3 addition on the microstructure and erosion wear of HVOF sprayed NiCrSiB coatings. *Mater. Res. Express* **2020**, *7*, 015006. [CrossRef]
15. Gualco, A.; Svoboda, H.G.; Surian, E.S. Effect of welding parameters on microstructure of Fe-based nanostructured weld overlay deposited through FCAW-S. *Weld. Int.* **2016**, *30*, 573–580. [CrossRef]
16. Saha, A.; Mondal, S.C. Multi-objective Optimization of Welding Parameters in MMAW for Nano-structured Hardfacing Mate-rial Using GRA Coupled with PCA. *Trans. Indian Inst. Met.* **2017**, *70*, 1491–1502. [CrossRef]
17. Aghakhani, M.; Naderian, P. Modeling and optimization of dilution in SAW in the presence of Cr_2O_3 nano-particles. *Int. J. Adv. Manuf. Technol.* **2015**, *78*, 1665–1676. [CrossRef]

18. Aghakhani, M.; Ghaderi, M.R.; Jalilian, M.M.; Derakhshan, A.A. Predicting the combined effect of TiO_2 nano-particles and welding input parameters on the hardness of melted zone in submerged arc welding by fuzzy logic. *J. Mech. Sci. Technol.* **2013**, *27*, 2107–2113. [CrossRef]
19. Chen, C.; Xue, H.; Chen, C.; Han, X.; Tang, H. Effect of nano oxide on microstructure and mechanical properties of low alloy high strength steel welds. *Hanjie Xuebao/Trans. China Weld. Inst.* **2016**, *37*, 29–34.
20. Liang, X.S.; Chen, C.X.; Peng, H.F. Effect of nano-scale titanium oxide on the microstructure of weld deposits for high strength low alloyed steel. *Cailiao Kexue Yu Gongyi/Mater. Sci. Technol.* **2009**, *17* (Suppl. S2), 41–45.
21. Hsu, P.W.; Chen, R.S.; Kao, F.H.; Tsai, S.Y.; Duh, J.G. Martensite nucleation site and grain refinement in duplex titanium alloy weldment by active flux with nanoparticle addition. *Sci. Technol. Weld. Join.* **2011**, *16*, 514–521. [CrossRef]
22. Bian, H.; Song, Y.; Liu, D.; Lei, Y.; Cao, J. Joining of SiO_2 ceramic and TC4 alloy by nanoparticles modified brazing filler metal. *Chin. J. Aeronaut.* **2020**, *33*, 383–390. Available online: https://www.researchgate.net/publication/333596700_Joining_of_SiO2_ceramic_and_TC4_alloy_by_nanoparticles_modified_brazing_filler_metal (accessed on 2 October 2023). [CrossRef]
23. Furkan; Kim, H.-J.; Lee, G.-H.; Jung, J.P. A Review of the Brazeability of Low-Temperature and Nano-Reinforced Al-Based Brazing Filler Metals. *J. Weld. Join.* **2022**, *40*, 216–224. [CrossRef]
24. Ahn, B. Recent Advances in Brazing Fillers for Joining of Dissimilar Materials. *Metals* **2021**, *11*, 1037. [CrossRef]
25. Tashev, P.; Kirilov, L.; Petrov, T.; Koprinkova-Christova, P.; Lukarski, Y. Optimization of the parameters for pulsed current tig remelting in nano modification of surface layers of structural steel parts. *Sci. Proc.* **2016**, *1*, 118–121.
26. Yang, J.; Hou, X.; Zhang, P.; Ren, X.; Yang, Q. Mechanical properties of the hypereutectoid Fe-Cr-C hardfacing coatings with different nano-Y2O3 additives and the mechanism analysis. *Mater. Sci. Eng.* **2016**, *655*, 346–354. [CrossRef]
27. Kuznetsov, M.A.; Zernin, E.A.; Danilov, V.I.; Zhuravkov, S.P.; Kryukov, A.V. Optimization of the modification parameters of a deposited metal by nanostructural fibers of the aluminium oxyhydroxide. *Nanotechnol. Russ.* **2018**, *13*, 521–530. [CrossRef]
28. Kuznetsov, M.A.; Zernin, E.A. Nanotechnologies and nanomaterials in welding production (review). *Weld. Int.* **2012**, *26*, 311–313. [CrossRef]
29. Lerner, M.I.; Svarovskaya, N.V.; Psah'e, S.G.; Bakina, O.V. Production technology, characteristics and some areas of application of electroexplosive metal nanopowders (Tekhnologiya polucheniya, kharakteristiki i nekotoryye oblasti primeneniya elektrovzryvnykh nanoporoshkov metallov). *Russ. Nanotechnologies (Ross. Nanotekhnologii)* **2009**, *4*, 56–68.
30. Zhuravkov, S.P.; Pustovalov, A.V.; Kuznetsov, M.A.; Rosliy, I.S.; Zernin, E.A. Assignment of Appropriate Conditions for Synthesizing Tungsten Nanopowder by Electric Explosion of Conductors. *IOP Conf. Ser. Mater. Sci. Eng.* **2016**, *142*, 012020. [CrossRef]
31. Golius, D.A.; Sokolov, E.G. Methods for producing tungsten nanopowders. In *Progressive Technologies in Modern Mechanical Engineering. Materials and Technologies of the XXI Century: Collection of Articles of the XVI International Scientific and Technical Conference, Penza, Russia, 24–25 June 2021*; Autonomous non-Profit Scientific and Educational Organization "Privolzhsky House of Knowledge": Penza, Russia, 2021; pp. 64–69.
32. Kolosov, V.N.; Miroshnichenko, M.N.; Orlov, V.M. Preparation of tungsten powders with a highly developed surface. *Chem. Technol.* **2021**, *22*, 153–160. [CrossRef]
33. Trufanov, D.Y.; Zobov, K.V.; Bardakhanov, S.P.; Gaponenko, V.R.; Chakin, I.K.; Domarov, E.V. Investigation of the effect of the type of starting material on the process of obtaining a yttrium oxide nanopowder by evaporation of a substance by a high-energy electron beam. *AIP Conf. Proc.* **2023**, *2504*, 030062. [CrossRef]
34. Yasuhara, S.; Orio, A.; Yasui, S.; Hoshina, T. Room temperature synthesis of $BaTiO_3$ nanoparticles using titanium bis(ammonium lactato) dihydroxide. *Jpn. J. Appl. Phys.* **2024**, *63*, 09SP16. [CrossRef]
35. Kilanski, L.; Lewinska, S.; Slawska-Waniewska, A.; Pavlović, V.B.; Filipović, S. Attempts to obtain $BaTiO_3/Fe_2O_3$ core-shell type structures: The role of iron oxide nanoparticle formation and agglomeration. *Inorg. Chem. Commun.* **2022**, *145*, 109960. [CrossRef]
36. Andreev, P.V.; Alekseeva, L.S.; Rostokina, E.E.; Drozhilkin, P.D.; Balabanov, S.S.; Murashov, A.A.; Karazanov, K.O. Synthesis of Si_3N_4-Based Powder Composites for Ceramic Fabrication by Spark Plasma Sintering. *Inorg. Mater.* **2022**, *58*, 1098–1104. [CrossRef]
37. Devi, K.N.; Vadivel, S. Room temperature fiber optic gas sensor technology based $Zn_3(VO_4)_2$/PMMA hybrid composites via facile hydrothermal route. *Opt. Fiber Technol.* **2024**, *82*, 103642. [CrossRef]
38. Velmurugan, G.; Kumar, S.S.; Chohan, J.S.; Kumar, A.J.; Manikandan, T.; Raja, D.E.; Saranya, K.; Nagaraj, M.; Barmavatu, P. Experimental Investigations of Mechanical and Dynamic Mechanical Analysis of Bio-synthesized CuO/Ramie Fiber-Based Hybrid Biocomposite. *Fibers Polym.* **2024**, *25*, 587–606. [CrossRef]
39. Kovziridze, Z.; Kapanadze, M.; Daraxvelidze, N.; Mshvildadze, M.; Nijaradze, N.; Balakhashvili, M.; Tabatadze, G.; Cheishvili, T. Smart Nanocomposite in the SiC-Si-Al-Al_2O_3-Geopolymer System. *Int. J. Innov. Res. Multidiscip. Educ.* **2024**, *3*, 1121–1136. [CrossRef]
40. Samokhin, A.; Alekseev, N.; Dorofeev, A.; Fadeev, A.; Sinaiskiy, M. Production of Spheroidized Micropowders of W-Ni-Fe Pseudo-Alloy Using Plasma Technology. *Metals* **2024**, *14*, 1043. [CrossRef]
41. Shan, X.; Cong, M.; Lei, W. Effect of Cladding Current on Microstructure and Wear Resistance of High-Entropy Powder-Cored Wire Coating. *Metals* **2022**, *12*, 1718. [CrossRef]
42. *GOST 5639*; Steels and Alloys. Methods for Detection and Determination of Grain Size. Gosstandart: Minsk, Belarus, 2023.
43. Kumar, S.S.; Murugan, N.; Ramachandran, K.K. Microstructure and mechanical properties of friction stir welded AISI 316L austenitic stainless steel joints. *J. Mater. Process. Technol.* **2018**, *254*, 79–90. [CrossRef]

44. Guo, J.; Liu, Z.; Su, Y. Effect of B on Microstructure and Properties of Surfacing Layer of Austenitic Stainless Steel Flux Cored Wire. *Materials* **2022**, *15*, 5884. [CrossRef] [PubMed]
45. Ai, X.; Liu, Z.; Zou, Z.; Wang, Z. Effect of Nano-Y_2O_3 on the Microstructure and Properties of WC-Reinforced Ni-Based Composite Surfacing Layer. *Materials* **2022**, *15*, 1665. [CrossRef] [PubMed]
46. Ai, X.; Liu, Z.; Zou, Z. Effect of Nano-Y_2O_3 on the Microstructure and Properties of Fe-Cr-C-N-Al Surfacing Alloy. *Crystals* **2023**, *13*, 1023. [CrossRef]